SPATIO-TEMPORAL EVOLUTION OF THE AIR POLLUTION SPECTRUM IN CHINA AT THE PREFECTURE LEVEL (2015-2020)

WANG, S. X.[1] – LI, J. M.[2*] – HAN, X. L.[2]

[1]*School of Economics, Shanxi Vocational University of Engineering Science and Technology, 369 Wenhua Street, Jinzhong, 030619, China*

[2]*School of Statistics, Shanxi University of Finance and Economics, 696 Wucheng Road, Taiyuan 030006, China*
(e-mail: wangsixian94@163.com; hanxl@sxufe.edu.cn)

**Corresponding author*
e-mail: lijm@sxufe.edu.cn

(Received 21st Sep 2024; accepted 17th Jan 2025)

Abstract. Air pollution is a critical global issue affecting human health. This paper introduces the Air Pollution Spectrum (APS), a multi-pollutant evaluation model (CO, NO_2, PM_{10}, $PM_{2.5}$, O_3, and SO_2) that surpasses the Air Quality Index (AQI) by reflecting both spatial quality and pollutant structure. This paper uses the Bayesian space-time hierarch piecewise regression model (BSTHPRM) to study the spatio-temporal evolution characteristics of the APS in China at the prefecture level (2015-2020). At the same time, the spatio-temporal characteristics of the APS component structure are also explored. We found higher levels of air pollution in Central, North, Northwest, and East China and lower air pollution levels in Southwest, South, and Northeast China. The change in APS values in Chinese cities during the study period is divided into two stages: in the first stage, the local change trend is rapid in Northwest, Southwest, and North China and slow in Central and Northeast China; in the second stage, the local change trend is fast in Northeast China and slow in Northwest and Southwest China. Spatial distribution and variation trends suggest that regional differences in APS values are narrowing. The APS component structure also has significant spatio-temporal distribution characteristics. O_3 has gradually become one of the main pollutants involved in air pollution, and its importance is greater in North China, West China, and South China and smaller in Central China and East China. PM_{10} accounts for the largest, most stable proportion of air pollution in China and, in general, plays an important role in air pollution in most regions except some western regions. The importance of $PM_{2.5}$ in air pollution in China has declined, with its importance greater in the central and eastern regions and smaller in the northern, western, and southern regions. The component structure of air pollutants at the prefecture level in China is changing significantly, with pollutants becoming more diverse. Parallel research on multiple pollutants has become an inevitable trend in air pollution research.
Keywords: *complex air pollution, spatio-temporal evolution, Bayesian statistics, air pollution values, air pollution component structure*

Introduction

Air pollution is one of the most pressing environmental health issues facing humanity worldwide. The 2021 WHO Global Air Quality Guidelines highlighted that air pollution exposure leads to significant global health losses, causing millions of deaths and reduced healthy life years annually (WHO, 2021). Air pollutants stimulate pro-inflammatory responses in immune cells, including macrophages, neutrophils, dendritic cells, and lymphocytes (Glencross et al., 2020). There is a relationship between air pollutants such as ozone (O_3), nitrogen dioxide (NO_2), and particulate matter (PM) and asthma exacerbations, respiratory morbidity, and mortality in people with chronic obstructive pulmonary disease (COPD) (Kelly and Fussell, 2011). Both $PM_{2.5}$ and PM_{10} air pollution are significantly related to adverse health effects, such as heart disease, stroke, blood pressure, and cardiovascular disease (Lee et al., 2014). Carbon monoxide (CO) is a highly

http://www.aloki.hu ● ISSN 1589 1623 (Print) ● ISSN 1785 0037 (Online)
DOI: http://dx.doi.org/10.15666/aeer/2302_25032525

reactive compound that prevents oxygen from being absorbed into the bloodstream, causing dizziness, confusion, and death at high concentrations (Graber et al., 2007). Sulfur dioxide is a severe respiratory irritant associated with increased inflammation of the respiratory tract (Samal et al., 2019). According to Energy and Air Pollution, in terms of the lethal factors for humans worldwide, China ranked fourth for air pollution (Wang et al., 2017). Accordingly, the Chinese air pollution problem deserves greater attention.

There are strong, complex links among air pollutants. Researchers found significant correlation characteristics between concentrations of $PM_{2.5}$ and PM_{10}, SO_2, NO_2, O_3, and CO (Li et al., 2014, 2016). It was also found that $PM_{2.5}$ responds to CO and O_3, with $PM_{2.5}$ having a strong positive correlation with CO (Fu et al., 2020). Synergies or antagonism between air pollutants can lead to complex nonlinear relationships between secondary aerosols and their precursors (Chu et al., 2016, Ma et al., 2018), such as the strong correlation between $PM_{2.5}$ and NO_2 concentrations during haze events (He et al., 2014) as well as O_3 and $PM_{2.5}$ reductions from a decrease in gas precursors (Chu et al., 2020). The common-origin, secondary nature of ground-level ozone and $PM_{2.5}$ and their precursor interactions make their formation strongly coupled (Liao et al., 2008). Sulfur dioxide emissions (e.g., coal burning, ocean transportation, etc.) have a relatively high contribution to PM (Liao et al., 2008). NO_2 and SO_2 have a synergistic effect when reacting on the surface of mineral dust (He et al., 2014; Ma et al., 2018). In addition to the direct oxidation of SO_2 in the atmosphere by O_3 and NO_2, O_3 and NO_2 in the atmosphere will also react (Zhang et al., 2021). To consider the combined relationship between air pollutants, summarizing the air quality status of complex mixtures of multiple pollutants into a number (e.g., a color pictogram or numerical representation), such as via the AQI, is beneficial for research and facilitates the accessible presentation of information to the public. An air pollutant is not independent but closely linked with other air pollutants and should be considered as a whole when considering air pollution. At this stage, there are very few studies considering the internal relationship of multiple pollutants and jointly judging their degree of air pollution. It is thus necessary to establish a comprehensive measure of air pollution that includes information on multiple air pollutants.

This paper revises the AQI and proposes the Air Pollution Spectrum (APS), a new air pollution measurement index encompassing multiple pollutants. The APS constructed in this paper contains six major air pollutants (CO, NO_2, PM_{10}, $PM_{2.5}$, O_3, and SO_2) at this stage and can not only reflect the spatial quality but also the component structure among the major pollutants. The APS has more advantages than the AQI in terms of the amount of information given about the pollutants and the differences between the reaction regions. China is a region with relatively serious air pollution. Thus, it is of great significance to explore the degree and component structure of air pollution at a Chinese prefecture level. Based on the BSTHPRM (Bayesian Space-Time Hierarchical Piecewise Regression Model) with an adaptive detection of local time inflection points and considering a spatial correlation, the spatio-temporal evolution characteristics of the APS values in China at the prefecture level during 2015-2020 were studied. At the same time, the spatio-temporal characteristics of the APS component structure were also explored. To comprehensively understand the status of air pollution and the composition of air pollutants in China, it is essential to consider the changes in the main air pollutants as well as minor air pollutants in various regions. This paper has two research purposes: to define the air pollution spectrum and present the calculation method used therein and to discover the temporal and spatial evolution characteristics (i.e., value and structure) of this spectrum at the prefecture level in China.

http://www.aloki.hu ● ISSN 1589 1623 (Print) ● ISSN 1785 0037 (Online)
DOI: http://dx.doi.org/10.15666/aeer/2302_25032525

Data and methodologies

Data source

This study used observed air quality data from prefectures in mainland China for the period of 2015-2020. As early as January 2013, the Ministry of Environmental Protection of China (MEPC) started to grant access to air quality data (including $PM_{2.5}$, PM_{10} [particulate matter with an aerodynamic diameter less than 10 mm], O_3, NO_2, SO_2, and CO) at the national air quality monitoring sites of some major cities (http://datacenter.mep.gov.cn/). This study uses urban air quality monitoring data published by the Chinese Ministry of Ecology and Environment on its website (http://www.cnemc.cn/), which has been publishing national air quality data since 13 May 2014. The air quality monitoring stations of China included 946 sites in 190 cities in 2014, 1494 sites in 367 cities in 2015, 1497 sites in 367 cities in 2016, 1563 sites in 368 cities in 2017, 1601 sites in 369 cities in 2018, 1633 sites in 369 cities in 2019, and 1641 stations in 367 cities in 2020. In addition, we calculated the annual average of the air quality data (including $PM_{2.5}$, PM_{10}, O_3, NO_2, SO_2, and CO; i.e., the annual arithmetic mean of the arithmetic mean of the natural 24-h day monitoring values) as the air pollutant values. Values from observations at sites with fewer than 20 h in a day, 27 days in a month (25 in February), or 324 days in a year were eliminated when calculating the annual average air pollutant concentrations (data sharing: https://github.com/wang-xiaoxian/wsx/blob/main/data.xlsx). The original data involved in this article totals 4,418,070 pieces. After the above data selection requirements, 4,278,552 pieces of data remain after cleaning, and the cleared data accounts for 3.16%. Additionally, this study covers 337 cities in China. The green areas on the map in *Figure 1* represent the prefecture-level cities included in the analysis.

Figure 1. *Map of the 337 prefecture-level cities in China*

http://www.aloki.hu ● ISSN 1589 1623 (Print) ● ISSN 1785 0037 (Online)
DOI: http://dx.doi.org/10.15666/aeer/2302_25032525

Research methods for the air pollution spectrum (APS)

This paper introduces the Air Pollution Spectrum (APS), a multi-pollutant evaluation model (CO, NO_2, PM_{10}, $PM_{2.5}$, O_3, and SO_2) that surpasses the Air Quality Index (AQI) by reflecting both spatial quality and pollutant structure. Both the APS and AQI consist of data simplifying the routinely monitored concentrations of several air pollutants into conceptual index values. Both are capable of providing a quantitative description of air quality, but the APS has more advantages: (1) The APS is a multi-pollutant-weighted comprehensive air quality evaluation model that assigns weights to six major air pollutant quality sub-indices and then sums them, providing the basis for determining the degree of local pollution by assigning larger weights to major pollutants and smaller weights to minor pollutants. The AQI only provides information on the primary pollutants. (2) The AQI can reflect the air quality level simply and intuitively, but it does not consider the correlation between multiple pollutants nor reflect the component structure of the six major air pollutants, while the APS can not only reflect the air quality condition and the contribution rate of each pollutant at different times and in different areas but also fully consider the association between each pollutant and other atmospheric pollutants. (3) Compared with the AQI, the APS can better reflect the difference in air pollution between regions. The following section specifies the steps for building the APS (three steps) and gives examples of the index's advantages. The APS is defined as the air pollution comprehensive measurement index, which is the weighted sum of the Individual Air Quality Index (IAQI) of the six major atmospheric pollutants—that is, the sum of each IAQI value ($IAQI_{CO}$, $IAQI_{NO_2}$, $IAQI_{O_3}$, $IAQI_{PM_{10}}$, $IAQI_{PM_{2.5}}$, $IAQI_{SO_2}$) multiplied by the weight of each element (*Fig. 2*).

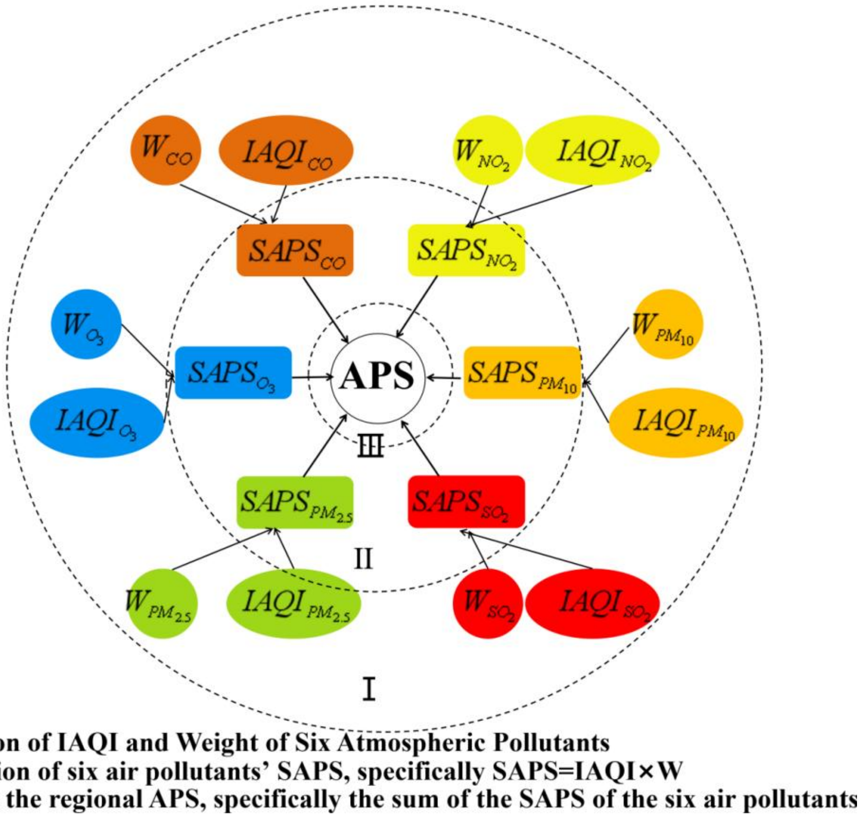

Figure 2. *Composition diagram of the APS*

http://www.aloki.hu ● ISSN 1589 1623 (Print) ● ISSN 1785 0037 (Online)
DOI: http://dx.doi.org/10.15666/aeer/2302_25032525

The following section will expand on the study of the atmospheric pollution spectrum and its spatio-temporal evolution characteristics. This paper employs the Exceedance Multiplier Method and the concept of comprehensive index construction to develop the APS, using Python for implementation. Next, the APS is analyzed using the Bayesian Space-Time Hierarchical Piecewise Regression Model to explore its spatio-temporal evolution, with WinBUGS software employed for the analysis. Finally, the spatio-temporal evolution of the APS structure is analyzed using Python. Regarding map display, this paper uses ArcGIS for graphical representation.

IAQI

We calculated the mean IAQI mean values for each prefecture from 2015 to 2020 using *Equation 1* according to the technical regulations of the ambient air quality index (HJ663-2013, 2013). The IAQI is the air quality index of each air pollutant, which are dimensionless.

$$IAQI_P = \frac{IAQI_{Hi} - IAQI_{Lo}}{BP_{Hi} - BP_{Lo}}(C_P - BP_{Lo}) + IAQI_{Lo} \quad \text{(Eq.1)}$$

where $IAQI_P$ is the index for pollutant p; C_P is the rounded concentration of pollutant p; BP_{Hi} is the threshold that is greater than or equal to C_P; BP_{Lo} is the threshold that is less than or equal to C_P; $IAQI_{Hi}$ is the AQI value corresponding to BP_{Hi}; and $IAQI_{Lo}$ is the AQI value corresponding to BP_{Lo}. The IAQI and corresponding thresholds of each pollutant are displayed in *Table 1*.

Table 1. *IAQI and corresponding thresholds of the six pollutants*

IAQI	**Sulfur dioxide (SO_2) ($\mu g/m^3$) [24 h]**	**Nitrogen dioxide (NO_2) ($\mu g/m^3$) [24 h]**	**Carbon monoxide (CO) ($\mu g/m^3$) [24 h]**	**Ozone (O_3) ($\mu g/m^3$) [8 h]**	**Particulate matter**	
					PM_{10} ($\mu g/m^3$) [24 h]	**$PM_{2.5}$ ($\mu g/m^3$) [24 h]**
0	0	0	0	0	0	0
50	50	40	2	100	50	35
100	150	80	4	160	150	75
150	475	180	14	215	250	115
200	800	280	24	265	350	150
300	1600	565	36	800	420	250
400	2100	750	48		500	350
500	2620	940	60		600	500

Establishing weights

In this paper, we use the Exceedance Multiplier Method, an objective weighting method that highlights the main factor[17], as the weight of the IAQI. It assigns different weights according to the difference in the contribution of different indicators in each evaluated object. In an “longitudinal” dynamic comprehensive evaluation, each indicator is weighted by the exceeding multiplier method, and the weight is normalized, which not only takes into account the relative importance of each pollutant of the evaluated object at different times but also the different pollutants. The essence is to determine the weight according to the principle that the pollution of the pollutant is low, the weight is small, and the pollution is high, the weight is large. The specific calculation is as follows:

http://www.aloki.hu ● ISSN 1589 1623 (Print) ● ISSN 1785 0037 (Online)
DOI: http://dx.doi.org/10.15666/aeer/2302_25032525

$$W_P = \frac{x_P / s_P}{\sum_{p=1}^{P} x_P / s_P} \quad \text{(Eq.2)}$$

W_P represents the weight value of the p-th pollutant; s_P represents the mean value of the five-level category standard for the p-th pollutant; and x_P represents the actual concentration of the p-th pollutant. In this paper, the reason for choosing the five classes of atmospheric pollutants as the criteria for calculating the weight of the air quality sub-index is that ozone (O_3) with an average 8-h concentration value above 800 $\mu g / m^3$ is no longer subject to its air quality sub-index calculation. If the existing six IAQI classes are used for the calculation of the IAQI weights, the relative importance of ozone (O_3) and its contribution to the APS will be exaggerated.

APS

Based on the above calculation of the IAQI value and its weights, it is possible to derive its component structure. Specifically, the APS value in the i-th region in the t-th year is equal to the sum of the IAQI value of the six major air pollutants and the product of the corresponding weights. The calculation formula is as follows.

$$APS = \sum_{p=1}^{P} IAQI_P \times W_P \quad \text{(Eq.3)}$$

$$SAPS_P = \frac{IAQI_P \times W_P}{\sum_{p=1}^{P} IAQI_P \times W_P} \quad \text{(Eq.4)}$$

$SAPS_P$ represents the proportion of the p-th pollutant in APS value for the i-th region in the t-th year. The sum of the six atmospheric pollutants' SAPS at the same time in the same area is a constant sum, which is 1.

The following are examples of the advantages of the APS. First, it is necessary to clarify the range of APS values. APS values are necessarily smaller than AQI values because AQI values only consider the primary pollutants and the calculation results in terms of the maximum values of the six IAQIs, while the APS is a combination of all the information on the six major pollutants and is a weighted value of the six air quality sub-indices.

Bayesian space-time hierarchical piecewise regression model

A developed Bayesian Space-Time Model was proposed by Li et al. (2019) and called a Bayesian Space-Time Hierarchical Piecewise Regression Model (BSTHPRM); it combines the ideas of the Bayesian Spatiotemporal Hierarchical Model BSTHM (Li et al., 2014) and the segmental regression model (Malash and El-Khaiary, 2010). The BSTHPRM not only incorporates spatial correlation into the spatial distribution characteristics of APS values but can also fully consider the diversification trend of APS values, capture the adaptive inflection point of the local trend, and explore the

http://www.aloki.hu ● ISSN 1589 1623 (Print) ● ISSN 1785 0037 (Online)
DOI: http://dx.doi.org/10.15666/aeer/2302_25032525

nonlinear local trend of APS values. The six-year data can be decomposed into three stages of change at most. According to the data characteristics of the Chinese APS values (2015-2020) and Ockham's Razor principle (Hoffmann et al., 1997; Gauch Jr, 2003), the local change trend can be divided into two stages. The mathematical form of the BSTHPRM proposed in this paper is as follows:

$$y_{it} \sim Normal(\mu_{M[\mathrm{i}],\mathrm{t}}, \sigma_y^2) \tag{Eq.5}$$

$$\log(\mu_{M[\mathrm{i}],t}) = \alpha + S_{M[\mathrm{i}]} + (b_0 t + \mathrm{v}_t) + b_{1,M[\mathrm{i}]} t + b_{2,M[\mathrm{i}]} (t - a_{1,M[\mathrm{i}]}) * G_{t,a_{1,M[\mathrm{i}]}} + \varepsilon_{M[\mathrm{i}],t} \tag{Eq.6}$$

$$G_{t,a_{1,M[\mathrm{i}]}} = \frac{1}{1 + e^{-\lambda(t - a_{1,M[\mathrm{i}]})}} \tag{Eq.7}$$

$$a_{1,M[\mathrm{i}]} \sim Uniform(2, \mathrm{T}-1) \tag{Eq.8}$$

$$\varepsilon_{M[\mathrm{i}],\mathrm{t}} \sim dnorm(0, prec.e) \tag{Eq.9}$$

$$K_{1,M[\mathrm{i}]} = b_{1,M[\mathrm{i}]} \tag{Eq.10}$$

$$K_{2,M[\mathrm{i}]} = b_{1,M[\mathrm{i}]} + b_{2,M[\mathrm{i}]} \tag{Eq.11}$$

$$SR_{M[\mathrm{i}]} = \exp(S_{M[\mathrm{i}]}) \tag{Eq.12}$$

where y_{it} is the annual average APS value of the i-th pixel at year t; $\mu_{M[\mathrm{i}],\mathrm{t}}$ is the mean parameter of the M[i]-th multiscale statistical unit; σ_y^2 is the corresponding variance; and α is the overall APS values of the mainland China prefectures during 2015-2020. $S_{M[\mathrm{i}]}$ is the local intercept terms of the M[i]-th multiscale statistical unit; $b_0 t + v_t$ describes the overall time trend containing a linear b_0 and a nonlinear tendency v_t, the prior distribution of which adopted a Gaussian distribution; $b_{1,M[\mathrm{i}]}$ and $b_{2,M[\mathrm{i}]}$ are local piecewise linear regression coefficients; and $a_{1,M[\mathrm{i}]}$ denotes the turning points of the M[i]-th multiscale statistical unit. The corresponding linear variation parameters are $k_{1,M[\mathrm{i}]}$ and $k_{2,M[\mathrm{i}]}$. The term $\varepsilon_{M[\mathrm{i}],\mathrm{t}}$ is a Gaussian noise error with a prior distribution assigned as a normal distribution $N(0, \sigma_\varepsilon^2)$. Through the BSTHPRM, the spatial relative magnitude of APS values in the M[i]-th multiscale statistical unit, denoted as $SR_{M[\mathrm{i}]}$, quantifying the APS pollution level relative to the overall level, can be estimated. The parameters $b_{1,M[\mathrm{i}]}$, $b_{2,M[\mathrm{i}]}$, and $a_{1,M[\mathrm{i}]}$ are considered simultaneously spatial, structured, and unstructured random effects through the assignment of the Bayesian image model (Besag et al., 1991). The construction of the three regression parameters is based on the conditional autoregressive (CAR)-normal prior of the first-order spatial adjacency matrix. The spatial correlation was established based on the topological relationships of multiscale statistical units. In this paper, the Bayesian statistical estimate was

http://www.aloki.hu ● ISSN 1589 1623 (Print) ● ISSN 1785 0037 (Online)
DOI: http://dx.doi.org/10.15666/aeer/2302_25032525

implemented by WinBUGS (Lunn et al., 2000) based on the Markov chain Monte Carlo (MCMC) algorithm. The convergence of the Bayesian inference results was judged by standard autocorrelation plots and trace plots.

Results

Descriptive statistical result

Studying the APS numerical levels of 337 cities in China during 2015-2020, it can be concluded that the spatial pattern of APS value is roughly stable (*Fig. 3*); however, certain differences were found between the study years, including obvious spatio-temporal trends. The area with the most serious APS pollution during 2015-2020 was Xinjiang, where Kashgar and Hotan exhibited the national air pollution peak areas in 2015–2016 and 2017–2020, respectively. Over the six years, the APS peaks reached 161.42 (i.e., Kashgar), 294.67 (i.e. Kashgar), 145.93 (i.e., Hotan), 245.75 (i.e., Hotan), 164.49 (i.e., Hotan) and 189.52 (i.e., Hotan), respectively. The area with the best APS quality in 2015–2020 was Inner Mongolia, with XilingolLeague and HulunBuir being the areas with the best air quality in the country in 2015–2016 and 2017–2020, respectively. Over the six years, APS values were 30.09 (i.e., XilingolLeague), 30.87 (i.e. XilingolLeague), 28.23 (i.e., HulunBuir), 23.81 (i.e., HulunBuir), 23.37 (i.e., HulunBuir) and 21.63 (i.e., HulunBuir), respectively.

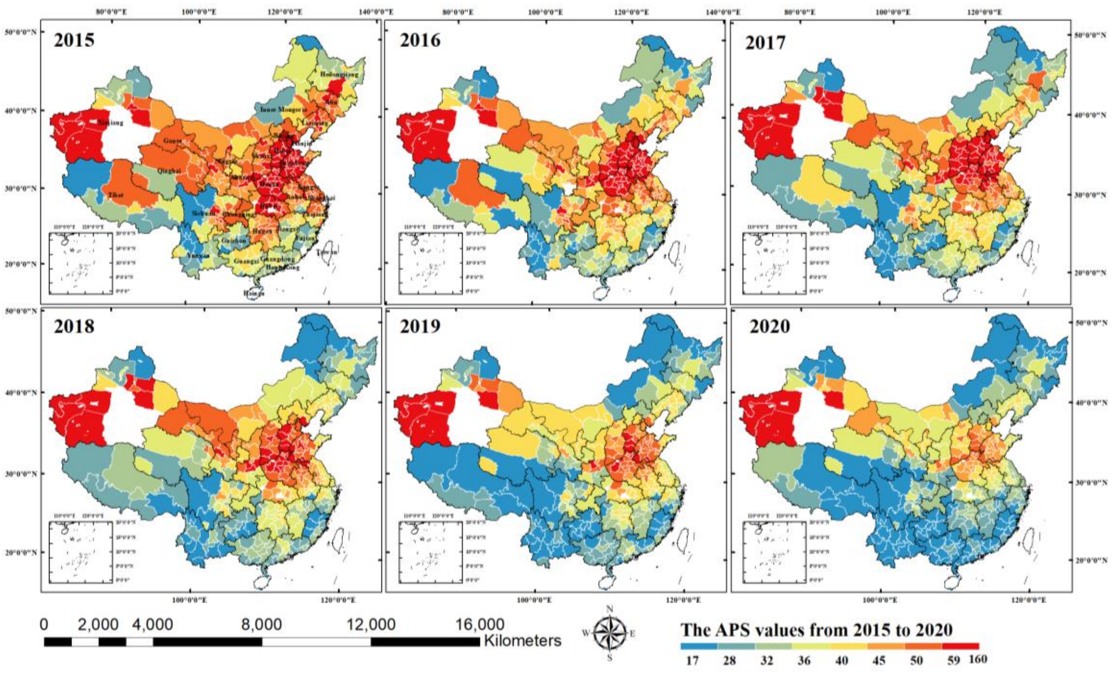

Figure 3. *Map of national annual average APS values during 2015-2020. Blank areas are areas where data is missing*

The APS values of Chinese cities have declined each year while the air quality has gradually improved during 2015-2020. The average APS values in Chinese cities over the six years were 51.47, 47.65, 45.10, 42.41, 38.65, and 35.02, respectively, demonstrating a decreasing trend with time (*Fig. 4*). The APS values corresponding to

http://www.aloki.hu ● ISSN 1589 1623 (Print) ● ISSN 1785 0037 (Online)
DOI: http://dx.doi.org/10.15666/aeer/2302_25032525

the seven major geographical divisions in China decreased by 25.35%–40.22%. Central China had the largest drop in the APS value (i.e.,40.22%), while Northwest China had the smallest drop in the APS value (i.e.,25.35%). At the same time, the APS levels in North China (the APS annual average:52.73), Central China (the APS annual average:50.45), and Northwest China (the APS annual average:52.25) were higher, and the APS levels in South China (the APS annual average:31.85), Southwest China (the APS annual average:32.79), and Northeast China (the APS annual average:38.19) are lower; meanwhile, the APS levels in East China (the APS annual average:44.63) and the whole country (the APS annual average:43.38) are comparable.

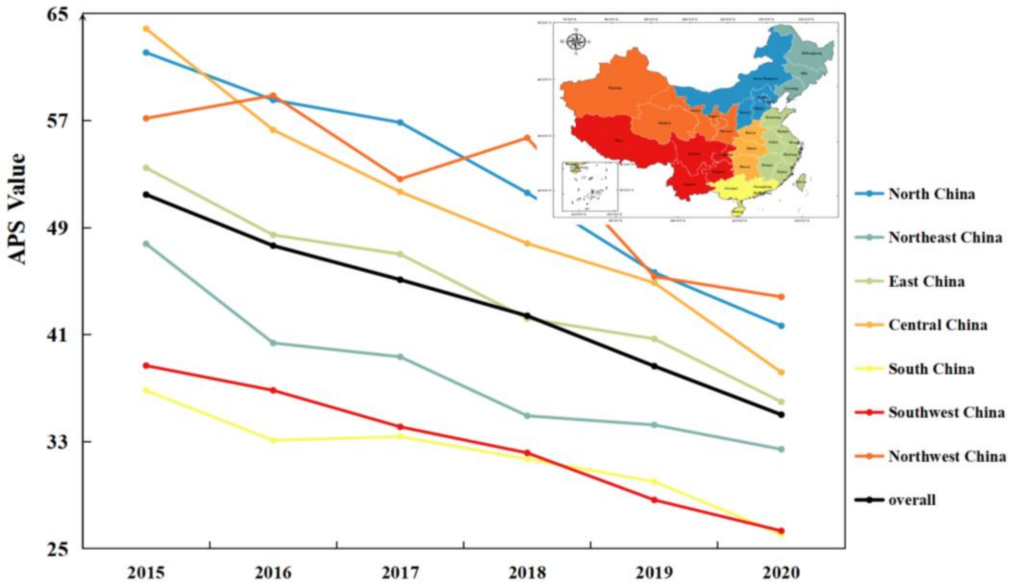

Figure 4. *Time series polyline of APS in China as a whole and for the seven geographical regions during 2015-2020*

Examples of APS advantages

Compared with the AQI, the APS can better reflect the difference in air pollution between regions. Specifically, the coefficients of variation (CV) of the APS values for the Chinese prefectures from 2015 to 2020 were 0.37, 0.45, 0.34, 0.43, 0.34, and 0.38, respectively, while the CVs of the AQI values for the prefectures were 0.3, 0.35, 0.28, 0.35, 0.29, and 0.31, respectively. Meanwhile, the APS value was necessarily larger than the arithmetic mean of the six IAQIs because the exceedance multiplier method was assigned a larger weight for important air pollutants and a smaller weight for minor air pollutants, highlighting the importance of heavy pollutants in the APS. The discrepancy between the APS and the AQI is mainly reflected in the fact that air pollution consists of a variety of major pollutants (e.g., the IAQI values of CO, NO_2, O_3, PM_{10}, $PM_{2.5}$, and SO_2 in Hotan in 2020 were 25.05, 34.07, 34.29, 195.18, 172.12, and 15.43, respectively, and the AQI was 195.18, while the APS had a value of 189.51. The APS assigned weights to the IAQI according to the importance of the atmospheric pollutants, the rapid industrialization of the Hotan area, and the main pollutants of $PM_{2.5}$ and PM_{10}, the weights of which were 52.19% and 48.63% respectively, while the AQI only considered the primary pollutant PM_{10} and set its PM_{10} to 100%. The variability in the APS and the IAQI expectations is mainly reflected in the presence of heavy

http://www.aloki.hu ● ISSN 1589 1623 (Print) ● ISSN 1785 0037 (Online)
DOI: http://dx.doi.org/10.15666/aeer/2302_25032525

pollutants in air pollution, (e.g., the IAQI values of CO, NO_2, O_3, PM_{10}, $PM_{2.5}$ and SO_2 in Ali in 2020 were 13.31, 14.61, 47.27, 14.33, 8.39, and 10.91, respectively, and the average value of IAQIs was 20.22, while the APS value was 32.71. The reason for this difference is that the green plants in the Ali area would release VOC during the peak growth period, which would then be directly or indirectly converted into ozone, at the same time, the highland cities had strong UV rays, which produced ozone by irradiating the ground and having an oxidizing effect on oxygen, resulting in a higher ozone concentration. The weight of ozone in the APS calculation was 59.63%.

Bayesian spatio-temporal statistical results

Based on the BSTHPRM, with posterior mean estimation of the steady-state spatial relative magnitude of the 337 Chinese cities, the APS values in China can generally be divided into three grades: cold spot, warm spot, and hotspot. In particular, the spatial units were identified as hot, warm, and cold spots when the posterior probability of $SR_{M[i]}$ $P(SR_{M[i]} > 1|y_{it})$ was > 0.80, between 0.20 and 0.80, and < 0.20, respectively (Richardson et al., 2004). Second, with posterior mean estimation of local trends in the 337 cities in China, the Chinese APS can be roughly divided into three levels: decreasing, stable, and increasing. Based on the posterior probability of the local trend parameters $P(K_{r,M[i]} > 0|y_{it})$ (r = 1, 2), the spatial units could also be classified into three categories: > 0.80, between 0.20 and 0.80, and < 0.20, respectively.

Overall spatial trends

The presented BSTHPRM in this paper estimated the overall spatial relative magnitude of the APS values, namely the overall spatial patterns, based on the simultaneous consideration of the space–time interaction during 2015-2020. The overall spatial trend—i.e., the overall relative spatial magnitude—of the APS from 2015 to 2020 was quantitatively described (*Fig. 5*) by the coefficient $SR_{M[i]}$, whose value indicated the magnitude of the APS in the multiscale subdivided grid, M[i], relative to the overall average level, $\exp(\alpha)$. Overall, the APS in Central China (Average value of $SR_{M[i]}$:1.18), North China (Average value of $SR_{M[i]}$:1.27), Northwest China (Average value of $SR_{M[i]}$:1.09), Northeast China (Average value of $SR_{M[i]}$:1.08) and East China (Average value of $SR_{M[i]}$:1.11) were relatively high, while those in Southwest China (Average value of $SR_{M[i]}$:0.78) and South China (Average value of $SR_{M[i]}$:0.77) were relatively low. This may be partly attributed to the fact that air pollution is influenced by climate and economy, with high greening in southern regions with high climatic rainfall and high traffic density and industrialization in economically developed regions.

About 40.06% of the cities in the country were considered to the APS hotspots, and these cities occupied 28.40% of the land area of Chinese cities. Northwest China accounted for the largest proportion of land area in the APS hotspots—about 37.82%. The APS hotspots in Shaanxi and Ningxia in Northwest China accounted for more than 60% of the total number of prefecture-level cities in each province, and the top two with the highest relative risk of the APS in Xinjiang were Hotan 2.41 (95%CI: 1.94, 2.87) and Kashgar 2.47 (95%CI: 2.05, 2.88). The specific implication expressed by the coefficient was that the air pollution levels in Hotan and Kashgar were respectively 2.41 and 2.47 times the national overall level. Moreover, 28.89% of the hotspots were from East China, which had the largest number of cities in hotspots. In East China, 92.31% of

http://www.aloki.hu ● ISSN 1589 1623 (Print) ● ISSN 1785 0037 (Online)
DOI: http://dx.doi.org/10.15666/aeer/2302_25032525

Jiangsu cities, 93.75% of Shandong cities, and 75% of Anhui cities were the APS hotspots. The spatial relative risk of the APS values corresponding to these cities was 1.08–1.71, indicating that the corresponding air pollution level was 1.08–1.71 times the national overall level.

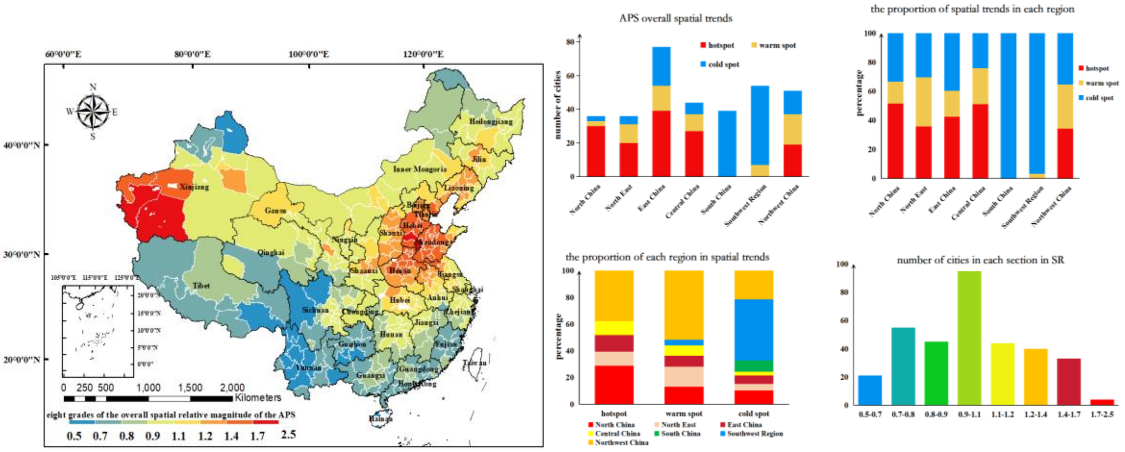

Figure 5. *The overall spatial, relative magnitudes (the posterior means of the parameter $SR_{M[i]}$) of the Chinese APS considering the space-time interaction during 2015-2020 based on the presented BSTHPRM*

About 18.99% of the cities in the country were considered to the APS warm spots, and warm spots accounted for 18.68% of the urban area in China. The proportion of cities and the proportion of land area in the warm spots in Northwest China were both the largest, with a ratio of 28.13% and 51.71%, respectively. All provinces in the Northwest were the APS warm spots. Among them, Gansu's APS temperature-spot area accounted for 71.43% of the total number of cities in the province, indicating that the level of air pollution was comparable to the overall level of the country.

About 40.95% of the cities in the country were considered to the APS cold spots, and cold spot areas occupied 52.49% of the land area of Chinese cities. More than one-third of the cities in the APS cold spots were concentrated in the southwest region, and these cities accounted for 45.66% of the land area in all cold spots. 66.67% of Sichuan cities and all areas of Chongqing, Guizhou, Yunnan, and Tibet were the APS cold spots. Among the top ten cities with the lowest spatial relative risk of APS values, six were occupied by the southwest region, represented by Diqing Tibetan Autonomous Prefecture 0.62 (95% CI: 0.51, 0.73), Dali Bai Autonomous Prefecture 0.65 (95% CI: 0.53, 0.78), and Qianxinan Buyi and Miao Autonomous Prefecture 0.65 (95% CI: 0.53, 0.78), which corresponded to air pollution levels 0.62, 0.65, and 0.65 times higher than the national overall level, respectively.

Local trends

Figure 6 illustrates the estimated result of the turning point of the local trend in the APS value in each multiscale statistical unit, namely parameter $a_{1,M[i]}$ of the BSTHPRM. The turning year equals 2014 plus the integer of $a_{1,M[i]}$—e.g., if $a_{1,M[i]}$ is 3.6, then the turning year is 2007. Specifically, the $a_{1,M[i]}$ of the 332 cities was 3, the two

http://www.aloki.hu ● ISSN 1589 1623 (Print) ● ISSN 1785 0037 (Online)
DOI: http://dx.doi.org/10.15666/aeer/2302_25032525

stages of the local APS values trends in these 332 cities were divided into 2015–2017 and 2018–2020; the $a_{1,M[i]}$ of the four cities of Naqu, Urumqi, and Kashgar was 2, the two stages of the local APS values trends in these cities were divided into 2015–2016 and 2017–2020; the $a_{1,M[i]}$ of Turpan and Hotan was 4, and the two stages of the local APS values trends in these cities were divided into 2015–2018 and 2019–2020. The local change trends of the two stages are further analyzed below.

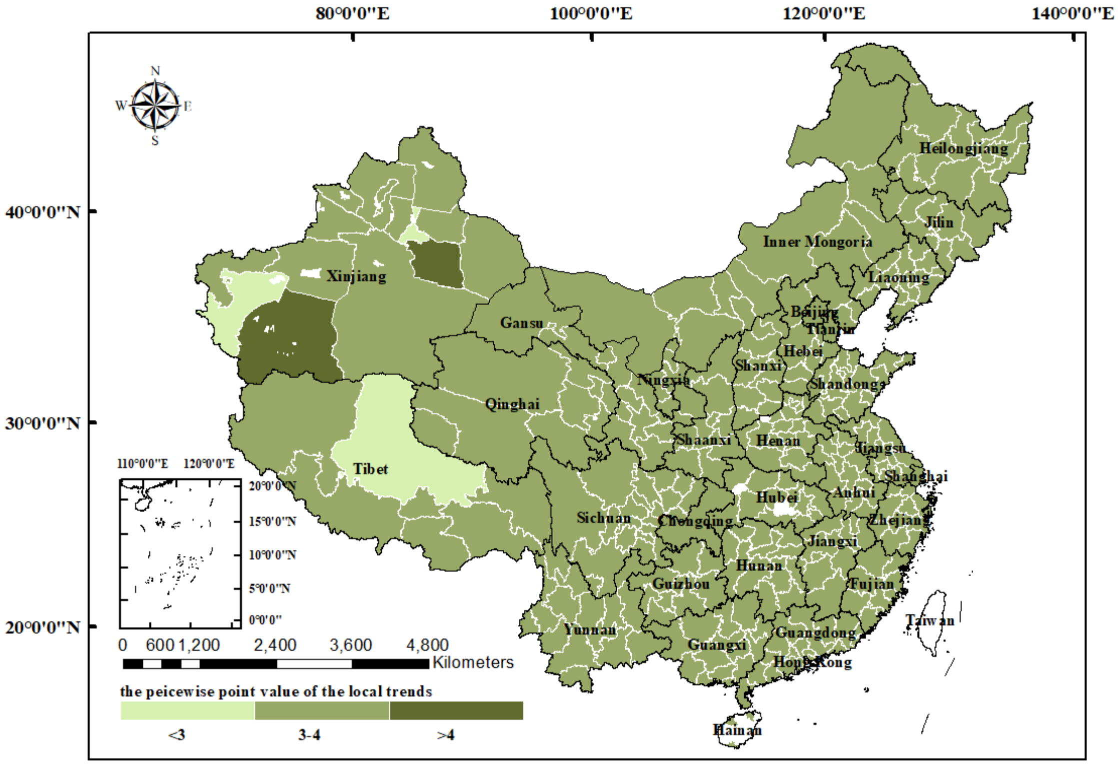

Figure 6. *Spatial distribution of the turning point of the local trend of the Chinese cities' APS; the posterior mean of the parameters,* $a_{1,M[i]}$ *; the turning year equals 2014 plus the integer of* $a_{1,M[i]}$

In the first stage, the local change trend in the APS values in Northwest China (Average value of $K_{1,M[i]}$: 0.03) and South China (Average value of $K_{1,M[i]}$: 0.01) was increasing, while the local change trend in the APS values in Central China (Average value of $K_{1,M[i]}$: -0.01) and Northeast China (Average value of $K_{1,M[i]}$: -0.02) was more strongly decreasing (*Fig. 7*). About 25.52% of the cities' APS in the country had an increasing in the first stage, where the APS value increasing accounted for 43.96% of the land area of Chinese cities. The proportion of cities and the proportion of land area in Northwest China with an increasing trend were both the largest at 40.70% and 57.66%, respectively. Among these northwest cities, the posterior probabilities of the local trend parameters $P(K_{r,M[i]} > 0 | y_{it})$ were greater than 0.8, and Xinjiang possessed nine of the top ten cities with the fastest APS values local change trend. The local change trend in the APS values corresponding to these cities were 0.06–0.13, indicating that the corresponding the air pollution spectrum pollution change speed was 1.06–1.14 times the national overall level. In the first stage, about 46.88% of the cities' APS in the country had a stable trend, accounting for about 37.19% of the land area of Chinese

http://www.aloki.hu ● ISSN 1589 1623 (Print) ● ISSN 1785 0037 (Online)
DOI: http://dx.doi.org/10.15666/aeer/2302_25032525

cities. Southwest China had the largest proportion of land area in the APS stable—about 36.33%. More than half of the cities in Yunnan, Guizhou, and Sichuan were considered to the APS stable. There was no significant difference in the rate of change and overall level of urban air pollution. About 27.60% of the cities' APS in the country had a decreasing trend in the first stage, accounting for 18.85% of the land area of Chinese cities. The decreasing trends of the APS were mainly concentrated in Northeast China and North China. In 75% of Northeast China cities, the posterior probabilities of the local trend parameters $P(K_{r,M[i]} > 0 | y_{it})$ were less than 0.2, and North China accounted for half of the top ten cities with the smallest APS values local change trend.

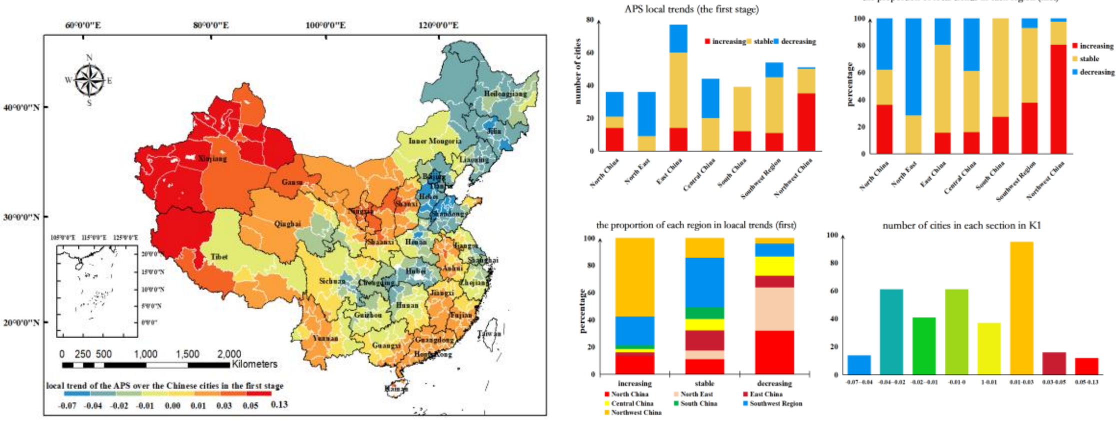

Figure 7. *Spatial pattern of the first-stage local trends (the posterior means of the parameter, $K_{1,M[i]}$) of the Chinese cities' APS from 2015 to the turning year, 2014 plus the integer of $a_{1,M[i]}$*

In the second stage, the local growth trend in the APS value in Northeast China (Average value of $K_{2,M[i]}$: 0.17) and East China (Average value of $K_{2,M[i]}$: 0.03) was found to be increasing, while the local growth trend in Northwest (Average value of $K_{2,M[i]}$: -0.11), Central China (Average value of $K_{2,M[i]}$: -0.05) and Southwest China (Average value of $K_{2,M[i]}$: -0.03) was more strongly decreasing (*Fig. 8*). About 16.02% of the cities' APS in the country had an increasing trend in the second stage, and areas with a strong change accounted for 17.67% of the land area of Chinese cities. Northeast China is the representative in that the APS value showed an increasing trend, and the posterior probabilities of the local trend parameters $P(K_{r,M[i]} > 0 | y_{it})$ were more than 0.8. Northeast China accounted for 70% of the top ten cities with the fastest local APS changes. The highest yearly increases in Northeast China were 1.33 (95%CI: 1.01, 1.76) per year, 1.29 (95%CI: 1.04, 1.61) per year, and 1.28 (95%CI: 1.04, 1.57) per year. There were 212 cities' APS across the country that had a second-stage stable trend, accounting for nearly half of the land area of Chinese cities. A decreasing trend of the APS accounted for 32.39% of the land area of Chinese cities, with Northwest China representing 71.02% the decreasing trend. Among the top ten cities with the slowest local change trend of the APS, Northwest China represented 80%, namely Kashgar, Hotan, Kizilsu Kirgiz Autonomous, Aksu, Turpan, Urumqi, Xianyang, and Xi'an. The local change trends in APS values in cities were -0.58–-0.16, indicating that the corresponding change rates in air pollution were 0.56–0.85 times the national overall level.

http://www.aloki.hu ● ISSN 1589 1623 (Print) ● ISSN 1785 0037 (Online)
DOI: http://dx.doi.org/10.15666/aeer/2302_25032525

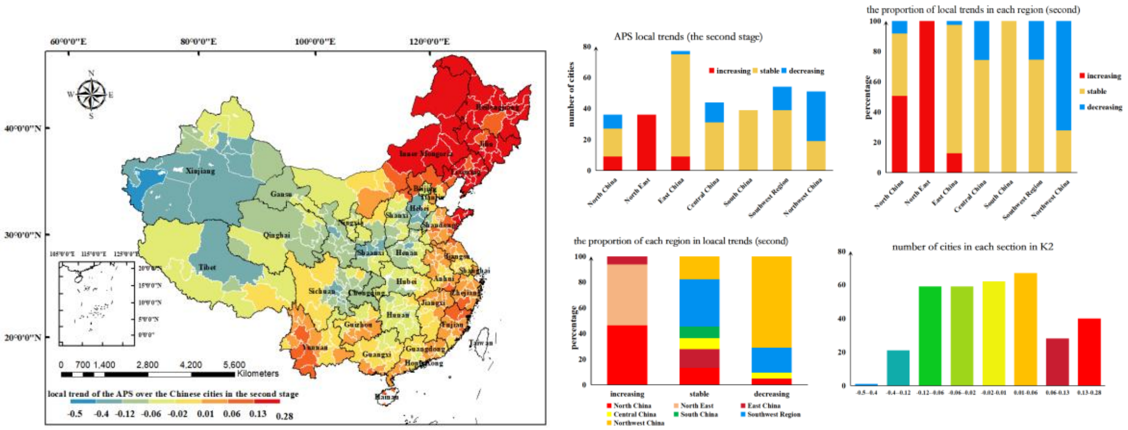

Figure 8. *Spatial pattern of second-stage local trends (the posterior means of the parameter, $K_{2,M[i]}$) of the Chinese cities' APS from the turning year, 2014 plus the integer of $a_{1,M[i]}$, to 2020*

The local APS values trends in China at the prefecture level were divided into two stages from 2015 to 2020 and showed opposite characteristics. One possible reason for this result is the change in China's industrial structure and energy consumption over the study period, such as the emphasis on industrial development and high energy consumption in Northwest China, Southwest China, and North China in the early period. Combined with the existing spatial distribution characteristics of the APS values, the opposing local variation trends between the two phases would lead to smaller spatial differences (*Table 2*).

Table 2. *Estimated values of the key parameters of the selected and representative multiscale statistical units*

Province	City	$SR_{M[i]}$ (95% CI)	$K_{1,M[i]}$ (95% CI)	$K_{2,M[i]}$ (95% CI)	$a_{1,M[i]}$
Inner Mongolia	XilingolLeague	0.91 (0.77, 1.09)	-0.01 (-0.04, 0.03)	0.16 (0.02, 0.33)	3.5
	HulunBuir	0.84 (0.66, 1.05)	-0.03 (-0.08, 0.02)	0.22 (-0.01, 0.44)	3.8
Beijing	Beijing	1.31 (1.10, 1.54)	-0.06 (-0.09, -0.02)	-0.03 (-0.20, 0.14)	3.6
Hebei	Xingtai	1.70 (1.46, 1.96)	-0.05 (-0.08, -0.02)	-0.14 (-0.28, -0.00)	3.4
	Baoding	1.59 (1.38, 1.82)	-0.06 (-0.09, -0.03)	-0.16 (-0.29, -0.02)	3.1
	Langfang	1.42 (1.19, 1.68)	-0.05 (-0.09, -0.02)	-0.04 (-0.21, 0.13)	3.6
	Hengshui	1.61 (1.37, 1.89)	-0.07 (-0.11, -0.04)	-0.13 (-0.28, 0.02)	3.3
Yunnan	Dali Bai	0.65 (0.53, 0.783	0.02 (-0.02, 0.06)	0.06 (-0.11, 0.25)	3.5
	Diqing Tibetan	0.62 (0.51, 0.74)	0.02 (-0.02, 0.06)	0.05 (-0.12, 0.21)	3.5
Tibet	Naqu	0.84 (0.73, 0.97)	0.00 (-0.04, 0.03)	-0.17 (-0.31, -0.03)	2.7
Guizhou	Qianxinan Buyi	0.65 (0.53, 0.78)	-0.01 (-0.05, 0.04)	0.04 (-0.13, 0.22)	3.5
Shaanxi	Xi'an	1.27 (1.08, 1.48)	0.02 (-0.01, 0.05)	-0.16 (-0.31, -0.02)	3.7
	Xianyang	1.30 (1.11, 1.51)	0.03 (0.01, 0.06)	-0.16 (-0.31, -0.02)	3.8
Xinjiang	Turpan	1.37 (1.12, 1.64)	0.06 (0.03, 0.10)	-0.22 (-0.40, -0.04)	4.1
	Hami	1.02 (0.84, 1.21)	0.06 (0.02, 0.09)	-0.07 (-0.25, 0.10)	3.6
	Changji	1.09 (0.91, 1.29)	0.06 (0.03, 0.10)	-0.14 (-0.32, 0.04)	3.9
	Bayingolin Mongolian	1.06 (0.90, 1.25)	0.05 (0.02, 0.08)	-0.15 (-0.28, -0.03)	3.5
	Aksu	1.69 (1.42, 1.99)	0.07 (0.03, 0.11)	-0.34 (-0.49, -0.19)	3.5
	Kizilsu Kirgiz	1.52 (1.24, 1.88)	0.09 (0.04, 0.15)	-0.37 (-0.60, -0.17)	3.9
	Hotan	2.41 (1.94, 2.87)	0.13 (0.10, 0.16)	-0.40 (-0.61, -0.25)	4.8
	Hi Kazak	0.93 (0.76, 1.10)	0.06 (0.02, 0.10)	-0.11 (-0.29, 0.06)	3.6
	Tacheng	0.75 (0.62, 0.89)	0.05 (0.02, 0.09)	-0.05 (-0.23, 0.13)	3.4

http://www.aloki.hu ● ISSN 1589 1623 (Print) ● ISSN 1785 0037 (Online)
DOI: http://dx.doi.org/10.15666/aeer/2302_25032525

APS component structure results

Time variation characteristics

In general, the APS of the prefecture-level cities in China during 2015-2020 showed strong temporal variability (*Fig. 9*). The importance of CO in terms of the APS of Chinese prefecture-level cities was relatively stable over the six years. From 2015 to 2016, the proportion of NO_2 in the APS of Chinese prefecture-level cities increased significantly, while its proportion has remained stable since 2016. The importance of O_3 in the APS of Chinese prefecture-level cities was found to first decrease and then increase, with the change in this proportion found to be relatively significant; O_3 gradually became one of the major pollutants in urban air pollution. PM_{10} accounted for the largest share of the APS, and it was relatively stable over the study period. The importance of $PM_{2.5}$ and SO_2 in the APS in Chinese cities decreased year by year, as reflected by their gradually decreasing values. In the literature, $PM_{2.5}$ has always been an important, mainstream air pollution research subject; however, through this study, we found that the importance of $PM_{2.5}$ in air pollution has been weakening each year, indicating that the parallel study of multiple pollutants has become an inevitable trend in air pollution research.

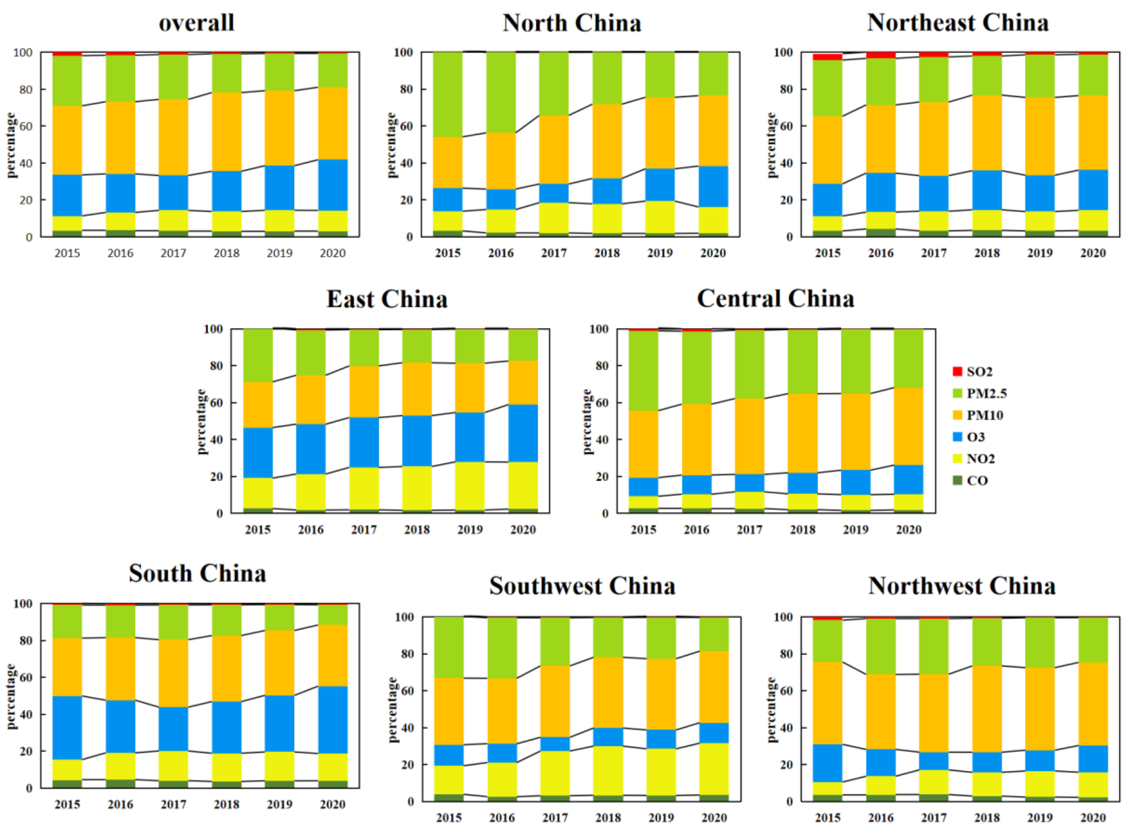

Figure 9. *The APS component structure map of overall China and the seven major geographic regions in China during 2015-2020*

The component structure of the APS in all regions of China had a more pronounced time-varying feature. In North China, the proportion of particulate matter in the APS changed significantly: the importance of $PM_{2.5}$ in air pollution decreased significantly each year, while PM_{10} gradually became the main pollutant, accounting for more than

http://www.aloki.hu ● ISSN 1589 1623 (Print) ● ISSN 1785 0037 (Online)
DOI: http://dx.doi.org/10.15666/aeer/2302_25032525

40%. The values of $PM_{2.5}$ and SO_2 as a percentage of the APS in Northeast China were found to decrease each year. Furthermore, the proportion of NO_2 in the APS in East China had a tendency to become larger each year, and $PM_{2.5}$ had a opposite change compared to NO_2, and the proportion of SO_2 in the APS first increased and then decreased. The importance of O_3 in the APS in Central China increased each year; meanwhile, the proportion of PM_{10} in the APS first increased and then gradually stabilized, becoming the main pollutant in air pollution. The proportion of NO_2 and PM_{10} in the APS in South China was increasing first and then gradually stabilizing, the importance of O_3 in APS was weakening first and then increasing, and the change of $PM_{2.5}$ was opposite. The importance of $PM_{2.5}$ in the APS decreased year by year in the Southwest China, and NO_2 had the opposite performance. The proportion of NO_2 in the APS in Northwest China first increased and then gradually stabilized, while the proportion of O_3 in the APS first decreased and then increased. The proportion of $PM_{2.5}$ in the APS first increased and then decreased, and the importance of SO_2 in the APS decreased. The conclusion is that the component structure of air pollutants has been undergoing major changes, with the main air pollutants tending to be diversified. In the context of regional air pollution research, the significance of single-pollutant research is continuously decreasing, while parallel research on multiple pollutants has become an inevitable trend.

The characteristics of the temporal changes in the APS component structure of the Chinese prefecture-level cities from 2015 to 2020 can be divided into two broad categories: the APS component structures is stable or highly variable (*Fig. 10*). For example, Huludao and Zhanjiang were cities with a stable APS component structure, with the ratio of each component in the APS not significantly changing during 2015-2020. Furthermore, the large changes in the component structure of the APS can be divided into two categories: changes in the major pollutant types in the APS and large changes in the proportion of air pollutants in the APS. For example, during the study period, the main air pollutant in Beijing changed from $PM_{2.5}$ to PM_{10} and the main air pollutant in Hulunbuir changed from PM_{10} to O_3. The major air pollutants in Suzhou and Hangzhou tended to be diversified, resulting in a high variability in pollutant values in the APS.

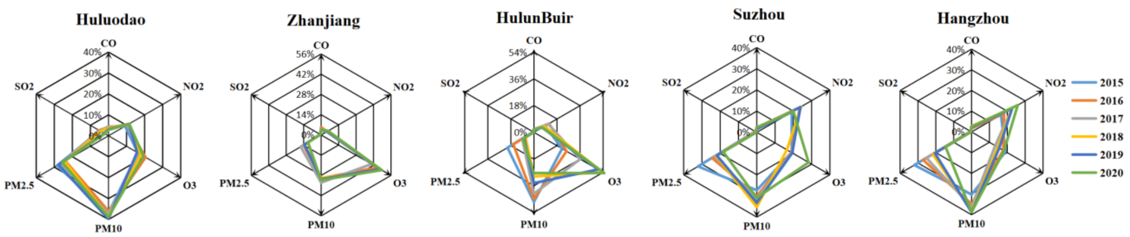

Figure 10. *The APS component structure change map of selected representative cities*

Spatial distribution characteristics

In general, the APS of the prefecture-level cities in China during 2015-2020 showed strong spatial variability (*Fig. 11*). The proportion of atmospheric pollutant CO in the APS in the southern region (accounting for 3.51%) was higher than that in the northern region (accounting for 2.82%). Moreover, the difference in the proportion of each pollutant in regions of higher atmospheric quality was reduced—i.e., the proportion of the atmospheric pollutant of CO (the most minor of the air pollutants) in the APS was significant in regions with small APS values. The spatial distribution of atmospheric

http://www.aloki.hu ● ISSN 1589 1623 (Print) ● ISSN 1785 0037 (Online)
DOI: http://dx.doi.org/10.15666/aeer/2302_25032525

pollutant NO_2 in the APS was higher in the eastern (accounting for 11.99%) and lower in the central regions (accounting for 9.32%); this was due to the large emissions of NO_2 in the eastern, which plays an important role in the APS component structure. The large proportion of O_3 in the APS in western (accounting for 26.09%) and southern China (accounting for 25.52%), the small proportion of O_3 in the APS in central (accounting for 18.88%) and northern China (accounting for 19.15%) stemmed from the strong radiation, long light hours, and high temperatures in western and southern China, which strongly contribute to the production of O_3. $PM_{2.5}$ in central (accounting for 26.48%) and northern China (accounting for 24.55%) accounted for a large proportion in the APS, while $PM_{2.5}$ in eastern (accounting for 22.83%), western (accounting for 18.18%) and southern China (accounting for 21.05%) accounted for a small proportion. $PM_{2.5}$ stems from daily power generation, industrial production, and automobile exhaust emissions. The central and eastern regions of China were undergoing high industrialization at the time and had correspondingly high $PM_{2.5}$ concentrations. Except for some western regions, PM_{10} took on an important role in air pollution in most of China, as indicated by its high proportion in the APS. The national share of SO_2 in the APS is all at a low level.

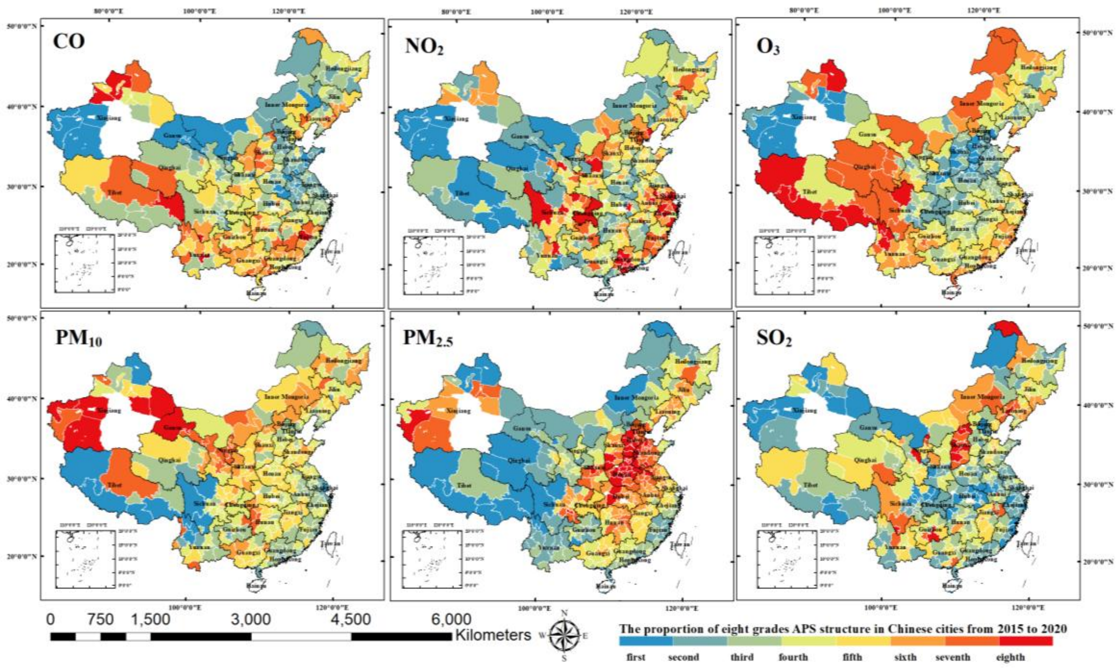

Figure 11. *Proportion of the six pollutants (including CO, NO_2, O_3, PM_{10}, $PM_{2.5}$, and SO_2) in the APS component structure of Chinese cities during 2015-2020 (the proportion is divided into eight levels and no specific numerical description is made)*

The structural characteristics of the APS for each city were mainly reflected in the variability of the main pollutant types in each region. PM_{10}, $PM_{2.5}$, O_3, and NO_2 were among the major pollutants in the APS of Beijing and Tianjin. Industrial production emissions, motor vehicle exhaust emissions, and the incremental increase in population were the main reasons for these high PM_{10}, $PM_{2.5}$, and NO_2 concentrations in Beijing and Tianjin. The main air pollutants in Northeast China as well as most cities of Shandong, Henan, Hebei, and Shanxi provinces were PM_{10} and $PM_{2.5}$, which are attributed to the fact

http://www.aloki.hu ● ISSN 1589 1623 (Print) ● ISSN 1785 0037 (Online)
DOI: http://dx.doi.org/10.15666/aeer/2302_25032525

that industrial production was still the dominant economic development model at the time of study. The main atmospheric pollutants in most Inner Mongolia cities were PM_{10} and O_3, with the change in O_3 concentration closely related to the weather situation. The main pollutant in South China was O_3. The lower cloudiness, higher temperature, and higher relative humidity in this area, along with the higher precursor concentrations, very small near-surface wind speeds, and predominantly radiative dispersion, resulted in large amounts of O_3 production. O_3 became the primary air pollutant in most cities in Yunnan and Tibet, and the unique topography of the Tibetan Plateau itself along with its dynamic and thermal effects represented one of the main reasons for the formation of a high-value area in terms of total O_3 over the Tibetan Plateau. The main pollutant in the atmosphere of most cities in Ningxia and Xinjiang was PM_{10}, which was mainly due to the frequent sand and dust storms in the two provinces and the high concentration of respirable particulate matter in the atmosphere due to sand and dust return.

Discussion

One of the greatest issues of our time is air pollution, not only because of its impact on climate change but also because of its impact on public and personal health (Manisalidis et al., 2020). Severe and persistent air pollution in China is an immense burden in terms of residents' health and financial wellbeing (Li et al., 2016). At the same time, a variety of air pollutants are not independent; instead, there are complex associations between air pollutants, where they interact with and transform each other. This is also the consideration and starting point of this paper: the linkage among atmospheric pollutants followed by the construction of an integrated measure of atmospheric pollutants (i.e., APS). It is necessary to establish a comprehensive measure of air pollution that includes information on multiple air pollutants. The APS constructed in this paper contains six major air pollutants (CO, NO_2, PM_{10}, $PM_{2.5}$, O_3, and SO_2) at this stage; it is essentially a multi-pollutant weighted comprehensive air quality evaluation model. The six atmospheric pollutants (CO, NO_2, PM_{10}, $PM_{2.5}$, O_3, and SO_2) each account for a certain proportion of the APS, where the sum of the weights is 1. Such an APS can reflect the atmospheric environmental quality conditions in different spatial and temporal conditions as well as the contribution rate of each pollutant and the component structure of atmospheric pollution. On this basis, in order to better understand the status of the air pollution spectrum in China, this paper investigated the spatial and temporal evolution characteristics of the APS value and APS component structure in Chinese cities during 2015-2020. We realized that the main air pollutants tend to be diversified at this stage and that it is of little significance to limit research to only one kind of pollutant for air pollution control. The parallel study of multiple pollutants will be the inevitable trend in air pollution research. In this paper, six major pollutants (CO, NO_2, PM_{10}, $PM_{2.5}$, O_3, and SO_2) were linked through the construction of the APS, and the results of the study can provide more practical references for Chinese policy considering multiple pollutants and synergistic air pollution control.

Unexpectedly, the region with the most serious air pollution in China is Xinjiang, which is also ignored by other articles, but it can also be reasonably explained. According to Xue's doctoral thesis (Xue, 2018), there are two factors that cause the above phenomenon: First, Xinjiang is the most resource-exporting region, and fossil energy enterprises have large emissions. The industrialization process will inevitably bring air pollution. Second, the area of extremely arid and arid areas accounts for 65.5%

http://www.aloki.hu ● ISSN 1589 1623 (Print) ● ISSN 1785 0037 (Online)
DOI: http://dx.doi.org/10.15666/aeer/2302_25032525

of the total area of Xinjiang. If the semi-arid areas are included, it accounts for 88.7% of the total area of Xinjiang. Due to water shortage, vegetation is sparse in large areas of Xinjiang (Fan et al., 2020). The vegetation coverage rate in northern Xinjiang is only about 0.3%, and the vegetation coverage rate in southern Xinjiang is less than 0.1%. The dry climate and desertification cause air pollution (Xue, 2018).

A general finding of previous studies is that O_3 has gradually become the main pollutant in the atmosphere (Feng et al., 2015; Lu et al., 2018; Wei et al., 2022; Ou et al., 2022). At the same time, the impact of SO_2 and NO_X in Chinese cities cannot be ignored (Zhao et al., 2018; Zhang et al., 2021). Therefore, the study of air pollution should not be limited to a single pollutant, but should integrate multiple pollutants to evaluate air pollution, which is also the necessity of writing this paper.

The literature consists of academic studies on overall air pollution that separately consider the six major air pollutants (CO, NO_2, PM_{10}, $PM_{2.5}$, O_3 and SO_2) and studies on the AQI. Comparatively, the APS study in this paper has certain advantages, such as (1) the APS is a total air pollutant research index that can directly determine the degree of regional air pollution, while the study of six pollutants separately lacks the determination of the overall air pollution. (2) The APS fully considers the linkages among atmospheric pollutants and regards them as a whole with internal correlations, while previous scholars deny these linkages and study them separately. (3) The APS can reflect the main and secondary relationships of air pollutants in each region for each time period, while previous studies have not provided this information. Moreover, compared with the existing scholars who studied the AQI, the APS study in this paper has certain advantages, such as, (1) according to the calculation principle, the APS includes information on six major air pollutants, while the AQI reflects information on only one pollutant. (2) The AQI can reflect the air quality level simply, while the APS can not only reflect the air quality condition and the contribution rate of each pollutant at different times and in different spaces but also fully consider the interaction between each pollutant and the component structure of air pollutants. (3) Compared with the AQI, the APS can better reflect the difference in air pollution between regions.

The APS constructed in this paper has profound implications for the study of air pollution, and the results of the study of the spatial and temporal evolution of APS value and the APS component structure will contribute to the policy planning of collaborative air pollution management. At the same time, the construction of APS is scalable, and it can be extended to global air pollution measurement, not only to explore the global air pollution level but also to explore the composition and structure of air pollution in various countries and regions. However, our study also has some limitations. First, the study needs a scientific and well-founded classification of air pollution levels based on APS values to help the public make an intuitive judgment about the air pollution situation. Furthermore, the APS can better reflect the differences in air pollution between regions than the AQI, but the APS requires rigorous mathematical proof.

Conclusion

Multi-pollutant air pollution (i.e., several pollutants reaching very high concentrations simultaneously) frequently occurs in many regions across China, it is necessary to construct a comprehensive index of air pollution (Hu et al., 2015). Many scholars have constructed indices to measure air pollution (Sowlat et al., 2011; Teologo et al., 2018; Haq, 2022; Zhang et al., 2022). This paper proposed an air pollution

http://www.aloki.hu ● ISSN 1589 1623 (Print) ● ISSN 1785 0037 (Online)
DOI: http://dx.doi.org/10.15666/aeer/2302_25032525

measurement index that contains information on various air pollutants, called the Air Pollution Spectrum (APS). Based on the BSTHPRM model with an adaptive detection of local time inflection points and considering spatial correlation, the spatio-temporal evolution characteristics of APS values in Chinese cities from 2015 to 2020 were studied. At the same time, compared with other scholars who only focus on the degree of air pollution, this paper also explores the structure of air pollution, and specifically studies the spatio-temporal evolution characteristics of the air pollution structure. We have reached the following preliminary conclusions.

Generally, the APS values of Chinese cities during 2015-2020 had significant spatial and temporal distribution characteristics, but the differences in the APS values between different regions were found to be decreasing over the study period. We found that the air pollution level was higher in Central China, North China, Northwest China, Northeast China and East China and lower in Southwest China and South China. Chinese cities' APS changes were divided into two phases during 2015-2020, and these two phases showed opposite characteristics. Many scholars often only study the temporal characteristics of air pollution (Li et al., 2017a; Fan et al., 2020; Zhou et al., 2021), and do not further study the regional characteristics under different time periods. This article does the above. Specifically, in the first stage, Northwest China and South China exhibited a faster trend of local change in air pollution, while Central China and Northeast China had a slower trend of local change in air pollution. In the second stage, Northeast China and East China had a faster local growth trend in air pollution, and Northwest China, Central China and Southwest China had a slower local growth trend in air pollution. The APS component structure also had significant spatio-temporal distribution characteristics. Many scholars focus on the spatio-temporal distribution of the absolute amounts of various pollutants (Li et al., 2017b; Fan et al., 2020; Lu et al., 2022), ignoring the spatio-temporal distribution of the structure of atmospheric pollutants when they are components. This article does the above. First, the atmospheric structure changed over time, with O_3 gradually becoming one of the main pollutants in urban air pollution, PM_{10} having the largest share in air pollution in Chinese cities but a relatively stable share in the APS, the importance of $PM_{2.5}$ in air pollution in Chinese cities decreasing each year, CO and NO_2 becoming less important in air pollution, and the share of SO_2 decreasing each year. Furthermore, the APS component structure also had distinct spatial characteristics. The proportion of CO in atmospheric pollution was higher in the south than in the north, and the spatial distribution of the importance of NO_2 in atmospheric pollution was found to be high in the east regions and low in the central regions. The importance of O_3 in atmospheric pollution was large in western and southern China, small in central and northern China. Additionally, the importance of $PM_{2.5}$ in atmospheric pollution was large in central and northern China, small in eastern, western, and southern China. PM_{10} took on an important role in air pollution in most of China, except for some western regions. SO_2 was of little importance in air pollution in the whole country. The types of major pollutants in each region have changed in addition to their proportions in the atmospheric structure.

Author contributions. Sixian Wang, Junming Li and Xiulan Han contributed to the study conception and design. Material preparation, data collection and analysis were performed by Sixian Wang. The first draft of the manuscript was written by Sixian Wang. Sixian Wang, Junming Li, Xiulan Han commented on previous versions of the manuscript. Sixian Wang, Junming Li and Xiulan Han read and approved the final manuscript.

Acknowledgements. The authors are grateful to all peer reviewers for their reviews and comments.

Funding. The authors declare that no funds, grants, or other support were received during the preparation of this manuscript.

Conflict of interests. The authors have no relevant financial or non-financial interests to disclose.

Availability of data and materials. All the data in the paper are drawn from Open Access and it is not involved in private or clinical data.

REFERENCES

[1] Besag, J., York, J., Mollié, A. (1991): Bayesian image restoration, with two applications in spatial statistics. – Annals of the Institute of Statistical Mathematics 43: 1-20.

[2] Chu, B., Zhang, X., Liu, Y., He, H., Sun, Y., Jiang, J., Li, J., Hao, J. (2016): Synergetic formation of secondary inorganic and organic aerosol: effect of SO_2 and NH_3 on particle formation and growth. – Atmospheric Chemistry and Physics 16(22): 14219-14230.

[3] Chu, B., Ma, Q., Liu, J., Ma, J., Zhang, P., Chen, T., Feng, Q., Wang, C., Yang, N., Ma, H., Ma, J. (2020): Air pollutant correlations in China: secondary air pollutant responses to NO_x and SO_2 control. – Environmental Science & Technology Letters 7(10): 695-700.

[4] Fan, H., Zhao, C., Yang, Y. (2020): A comprehensive analysis of the spatio-temporal variation of urban air pollution in China during 2014–2018. – Atmospheric Environment 220: 117066.

[5] Feng, Z., Hu, E., Wang, X., Jiang, L., Liu, X. (2015): Ground-level O_3 pollution and its impacts on food crops in China: a review. – Environmental Pollution 199: 42-48.

[6] Fu, H., Zhang, Y., Liao, C., Mao, L., Wang, Z., Hong, N. (2020): Investigating $PM_{2.5}$ responses to other air pollutants and meteorological factors across multiple temporal scales. – Scientific Reports 10(1): 1-10.

[7] Gauch Jr, H. G. (2003): Scientific Method in Practice – Cambridge University Press, Cambridge.

[8] Glencross, D. A., Ho, T. R., Camina, N., Hawrylowicz, C. M., Pfeffer, P. E. (2020): Air pollution and its effects on the immune system. – Free Radical Biology and Medicine 151: 56-68.

[9] Graber, J. M., Macdonald, S. C., Kass, D. E., Smith, A. E., Anderson, H. A. (2007): Carbon monoxide: the case for environmental public health surveillance. – Public Health Reports 122(2): 138-144.

[10] Haq, M. A. (2022): SMOTEDNN: a novel model for air pollution forecasting and AQI classification. – Computers, Materials & Continua 71(1).

[11] He, H., Wang, Y., Ma, Q., Ma, J., Chu, B., Ji, D., Tang, G., Liu, C., Zhang, H., Hao, J. (2014): Mineral dust and NO_x promote the conversion of SO_2 to sulfate in heavy pollution days. – Scientific Reports 4(1): 4172.

[12] HJ663-2013 (2013): Technical Regulation on Ambient Air Quality Index (on Trial). – Ministry of Environmental Protection of the Peoples Republic of China (MEP), Beijing.

[13] Hoffmann, R., Minkin, V. I., Carpenter, B. K. (1997): Ockham's razor and chemistry. – International Journal for the Philosophy of Chemistry 3: 3-28.

[14] Hu, J., Ying, Q., Wang, Y., Zhang, H. (2015): Characterizing multi-pollutant air pollution in China: comparison of three air quality indices. – Environment International 84: 17-25.

[15] Kelly, F. J., Fussell, J. C. (2011): Air pollution and airway disease. – Clinical & Experimental Allergy 41(8): 1059-1071.

[16] Lee, B. J., Kim, B., Lee, K. (2014): Air pollution exposure and cardiovascular disease. – Toxicological Research 30: 71-75.

[17] Li, G., Haining, R., Richardson, S., Best, N. (2014): Space–time variability in burglary risk: a Bayesian spatio-temporal modelling approach. – Spatial Statistics 9: 180-191.

http://www.aloki.hu ● ISSN 1589 1623 (Print) ● ISSN 1785 0037 (Online)
DOI: http://dx.doi.org/10.15666/aeer/2302_25032525

[18] Li, J., Han, X., M., Zhang, X., Wang, S. (2019): Globally analysing spatiotemporal trends of anthropogenic $PM_{2.5}$ concentration and population's $PM_{2.5}$ exposure from 1998 to 2016. – Environment International 128: 46-62.
[19] Li, Q., Wang, E., Zhang, T., Hu, H. (2017a): Spatial and temporal patterns of air pollution in Chinese cities. -Water, Air, & Soil Pollution 228: 1-22.
[20] Li, R., Cui, L., Li, J., Zhao, A., Fu, H., Wu, Y., Zhang, L., Kong, L., Chen, J. (2017b): Spatial and temporal variation of particulate matter and gaseous pollutants in China during 2014–2016. – Atmospheric Environment 161: 235-246.
[21] Li, S., Williams, G., Guo, Y. (2016): Health benefits from improved outdoor air quality and intervention in China. – Environmental Pollution 214: 17-25.
[22] Liao, K. J., Tagaris, E., Napelenok, S. L., Manomaiphiboon, K., Woo, J. H., Amar, P., He, S., Russell, A. G. (2008): Current and Future Linked Responses of Ozone and $PM_{2.5}$ to Emission Controls. – ACS Publications, Washington, DC.
[23] Lu, H., Xie, M., Liu, X., Liu, B., Liu, C., Zhao, X., Du, Q., Wu, Z., Gao, Y., Xu, L. (2022): Spatial-temporal characteristics of particulate matters and different formation mechanisms of four typical haze cases in a mountain city. – Atmospheric Environment 269: 118868.
[24] Lu, X., Hong, J., Zhang, L., Cooper, O. R., Schultz, M. G., Xu, X., Wang, T., Gao, M., Zhao, Y., Zhang, Y. (2018): Severe surface ozone pollution in China: a global perspective. – Environmental Science & Technology Letters 5(8): 487-494.
[25] Lunn, D. J., Thomas, A., Best, N., Spiegelhalter, D. (2000): WinBUGS-a Bayesian modelling framework: concepts, structure, and extensibility. – Statistics and Computing 10: 325-337.
[26] Ma, J., Chu, B., Liu, J., Liu, Y., Zhang, H., He, H. (2018): NO_x promotion of SO_2 conversion to sulfate: an important mechanism for the occurrence of heavy haze during winter in Beijing. – Environmental Pollution 233: 662-669.
[27] Malash, G. F., El-Khaiary, M. I. (2010): Piecewise linear regression: a statistical method for the analysis of experimental adsorption data by the intraparticle-diffusion models. – Chemical Engineering Journal 163(3): 256-263.
[28] Manisalidis, I., Stavropoulou, E., Stavropoulos, A., Bezirtzoglou, E. (2020): Environmental and health impacts of air pollution: a review. – Frontiers in Public Health 14.
[29] Ou, S., Wei, W., Cai, B., Yao, S., Wang, K., Cheng, S. (2022): Exploring the causes for co-pollution of O_3 and $PM_{2.5}$ in summer over North China. – Environmental Monitoring and Assessment 194(4): 289.
[30] Richardson, S., Thomson, A., Best, N., Elliott, P. (2004): Interpreting posterior relative risk estimates in disease-mapping studies. – Environmental Health Perspectives 112(9): 1016-1025.
[31] Samal, K. K. R., Babu, K. S., Das, S. K., Acharaya, A. (2019): Time series based air pollution forecasting using SARIMA and prophet model. – Proceedings of the 2019 International Conference on Information Technology and Computer Communications, Singapore.
[32] Sowlat, M. H., Gharibi, H., Yunesian, M., Mahmoudi, M. T., Lotfi, S. (2011): A novel, fuzzy-based air quality index (FAQI) for air quality assessment. – Atmospheric environment 45(12): 2050-2059.
[33] Teologo, A. T., Dadios, E. P., Baldovino, R. G., Neyra, R. Q., Javel, I. M. (2018): Air quality index (AQI) classification using CO and NO_2 pollutants: a fuzzy-based approach. – TENCON 2018-2018 IEEE Region 10 Conference, pp. 0194-0198.
[34] Wang, J., Zhang, Y., Liu, Z., Norris, P., Romero, C. E., Xu, H., Pan, W. P. (2017): Effect of coordinated air pollution control devices in coal-fired power plants on arsenic emissions. – Energy & Fuels 31(7): 7309-7316.
[35] Wei, J., Li, Z., Li, K., Dickerson, R. R., Pinker, R. T., Wang, J., Liu, X. Sun, L., Xue, W., Cribb, M. (2022): Full-coverage mapping and spatiotemporal variations of ground-level

http://www.aloki.hu ● ISSN 1589 1623 (Print) ● ISSN 1785 0037 (Online)
DOI: http://dx.doi.org/10.15666/aeer/2302_25032525

ozone (O3) pollution from 2013 to 2020 across China. – Remote Sensing of Environment 270: 112775.

[36] WHO (2021): WHO Global Air Quality Guidelines: Particulate Matter ($PM_{2.5}$ and PM_{10}), Ozone, Nitrogen Dioxide, Sulfur Dioxide and Carbon Monoxide: Executive Summary. – WHO, Geneva.

[37] Xue, T. (2018): An economic analysis of the supply chain and empirical study of the interactive mechanism of urbanisation, industrialisation and environment. – Doctoral dissertation, University of Southampton.

[38] Zhang, K., Wang, X. (2021): Pollution haven hypothesis of global CO_2, SO_2, NO_x—Evidence from 43 economies and 56 sectors. – International Journal of Environmental Research and Public Health 18(12): 6552.

[39] Zhang, Q., Tian, L., Fu, F., Wu, H., Wei, W., Liu, X. (2022): Real-time and image-based AQI estimation based on deep learning. – Advanced Theory and Simulations 5(6): 2100628.

[40] Zhang, S., Li, D., Ge, S., Liu, S., Wu, C., Wang, Y., Chen, Y., Lv, S., Wang, F., Meng, J. and Wang, G. (2021): Rapid sulfate formation from synergetic oxidation of SO_2 by O_3 and NO_2 under ammonia-rich conditions: implications for the explosive growth of atmospheric $PM_{2.5}$ during haze events in China. – Science of the Total Environment 772: 144897.

[41] Zhao, S., Liu, S., Hou, X., Cheng, F., Wu, X., Dong, S., Beazley, R. (2018): Temporal dynamics of SO_2 and NO_X pollution and contributions of driving forces in urban areas in China. – Environmental Pollution 242: 239-248.

[42] Zhou, D., Lin, Z., Liu, L., Qi, J. (2021): Spatial-temporal characteristics of urban air pollution in 337 Chinese cities and their influencing factors. – Environmental Science and Pollution Research 28: 36234-36258.

http://www.aloki.hu ● ISSN 1589 1623 (Print) ● ISSN 1785 0037 (Online)
DOI: http://dx.doi.org/10.15666/aeer/2302_25032525